

## **APPENDIX -I-**

### **Microstructural analysis by means of x-ray diffraction**

#### **I.I.- Bragg's law of x-ray diffraction**

To describe the way x-rays diffract in a perfect crystal (without distortions and with atoms located in fixed positions) we will consider that x-rays are perfectly parallel and monochromatic (with a wavelength  $\lambda$ ) and make an incident angle  $\theta$  with respect to the reticular planes of the crystal [1].

As a result of interactions with atoms, x-rays are dispersed in all directions, but the diffraction beam is formed from those x-rays for which the incident angle is equal to the reflected angle. For example, as can be seen in figure A1.1, the rays  $I$  and  $Ia$  strike atoms  $K$  and  $P$  and are scattered in all directions, but only in the directions  $I'$  and  $Ia'$  these scattered beams are completely in phase and therefore capable to reinforce one another (constructive interference). Therefore, the difference in their path length will fulfil the following relationship:

$$QK - PR = PK \cos \theta - PK \cos \theta = 0 \quad (\text{a1.1})$$

Similarly, the rays scattered by all the atoms in the first plane in a direction parallel to  $I'$  are in phase and also contribute to the diffracted beam. This will actually occur for all planes separately.

However, rays  $I$  and  $2$  will be scattered by atoms  $K$  and  $L$ , respectively, and their path difference will be:

$$ML + LN = d \sin \theta + d \sin \theta \quad (\text{a1.2})$$

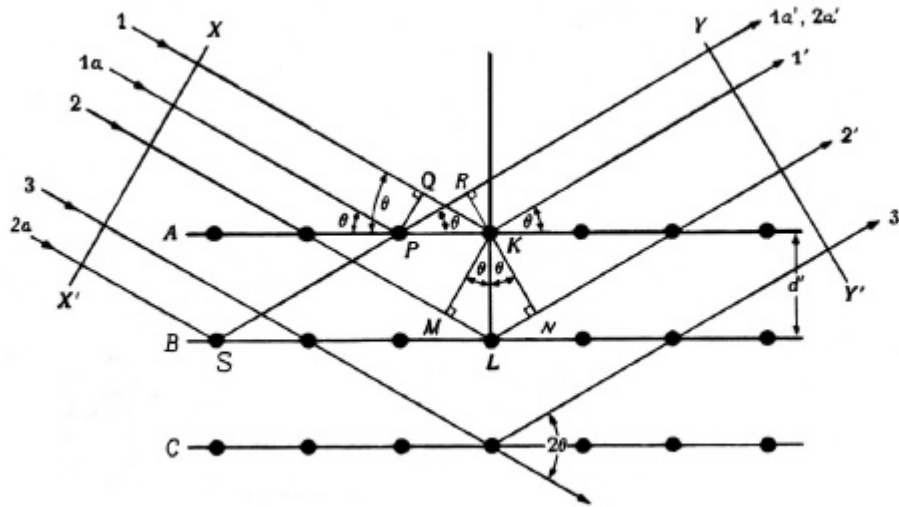


Figure A1.1: X-ray diffraction in a crystal [1].

Similar relationships can be derived from other rays striking atoms in different planes. Therefore, rays 1' and 2' will be completely in phase if the following relationship is fulfilled (difference of path length equal to a whole number of wavelengths,  $n$ ):

$$n\lambda = 2d \sin \theta \quad (\text{a1.3})$$

where  $n$  is the reflection order,  $d$  is the interplanar difference and  $\theta$  is the incidence angle. This relationship is known as Bragg's law, since it was elaborated in 1912 by W.L. Bragg [2].

**I.II.- The effect of crystallite size and microstrains on the XRD patterns: Scherrer's formula deduction**

Bragg's law of XRD assumes the crystal to be ideal, without defects. This is usually not fulfilled in reality. Moreover, x-rays are never perfectly collimated, i.e. some divergence is always inevitably present. This is of big importance, since it allows determination of the *crystallite size*, which is the minimum part of material that diffracts coherently [1].

Let us consider a crystal of finite thickness  $t$ , composed of a set of  $m + 1$  diffraction planes (see figure A1.2). In the figure,  $\theta$  is the incident variable angle,  $\theta_B$  is the incident angle

that fulfils exactly Bragg's law and  $\mathbf{l}$  and  $d$  are the wavelength of the incident beam and the interplanar distance, respectively.

The rays  $A, D, \dots, M$  make an incident angle with the crystallographic planes exactly equal to  $\mathbf{q}_B$ . The ray  $D'$  is out of phase with respect to  $A'$  by exactly an amount equal to one wavelength. And  $M'$  is  $m$  wavelengths out of phase with respect to  $A'$ . Therefore, the rays  $A', D', \dots, M'$  interfere constructively and form a diffracted beam of maximum intensity. Let us now suppose that two different rays,  $B$  and  $C$ , that make incident angles  $\mathbf{q}_1$  and  $\mathbf{q}_2$ , slightly different from  $\mathbf{q}_B$ , so that:

$$\begin{aligned}\mathbf{q}_1 &= \mathbf{q}_B + \Delta\mathbf{q} \\ \mathbf{q}_2 &= \mathbf{q}_B - \Delta\mathbf{q}\end{aligned}\tag{a1.4}$$

and fulfil the condition:

$$\begin{aligned}2t \sin\mathbf{q}_1 &= (m+1)\mathbf{l} \\ 2t \sin\mathbf{q}_2 &= (m-1)\mathbf{l}\end{aligned}\tag{a1.5}$$

Thus, for  $\mathbf{q}_1$ , the planes  $i$  and  $i + l$  are slightly out of phase and between the planes 0 and  $m$  it is possible to find midway in the crystal a plane for which the difference of phase with respect to  $B'$  will be exactly  $\mathbf{l} / 2$ , thus interfering destructively with it. These rays cancel each other and so do the other rays from similar pairs of planes throughout the crystal, the net effect being that rays scattered by the top half of the crystal cancel those scattered by the bottom half. The intensity of the beam diffracted at an angle  $\mathbf{q}_1$  is therefore zero. Similarly, the intensity of the beam diffracted at an angle  $\mathbf{q}_2$  is also zero. For rays making an incident angle between  $\mathbf{q}_1$  and  $\mathbf{q}_B$  the intensity will have an intermediate value between  $I_{Max}$  and  $I = 0$ . Thus, a distribution of intensities is obtained.

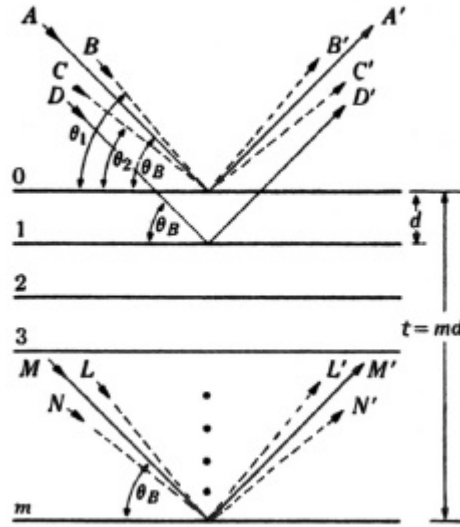


Figure A1.2: Finite crystallite size effect on diffraction [1]

Subtracting equations (a1.5) one obtains:

$$2I = 2t (\sin q_1 - \sin q_2) = 4t \cos \left( \frac{q_1 + q_2}{2} \right) \sin \left( \frac{q_1 - q_2}{2} \right) \approx 4t \left( \frac{q_1 - q_2}{2} \right) \cos q_B \quad (\text{a1.6})$$

where the approximation  $\sin(x) \approx x$  has been used, together with:

$$\frac{q_1 + q_2}{2} = q_B \quad (\text{a1.7})$$

If we define:  $(q_1 - q_2) = b$ , where  $b$  is the half-height width, from equation a1.6 one can deduce:

$$b = \frac{I}{t \cos q_B} \quad (\text{a1.8})$$

which is the well-known *Scherrer formula* for crystallite size [1,3]. A more precise treatment gives that:

$$\mathbf{b} = \frac{0.9\mathbf{l}}{t \cos \mathbf{q}_B} \quad (\text{a1.9})$$

This equation is valid only for crystallite sizes smaller than 100 nm. Moreover,  $t$  is not exactly the crystallite size but the *coherent diffraction domain* (portion of crystal that gives a beam of diffracted rays with well-defined phase relation). This means that dislocations or stacking faults inside the crystallites can also limit the *coherent diffraction domain*. Moreover, for an infinite crystal:

$$\lim_{m \rightarrow \infty} (\sin \mathbf{q}_1) = \lim_{m \rightarrow \infty} \left( \frac{m-1}{m} \frac{\mathbf{l}}{2d} \right) = \frac{\mathbf{l}}{2d} = \sin \mathbf{q}_B \quad (\text{a1.10})$$

This means that for an infinite crystal  $\mathbf{q}_1 = \mathbf{q}_B = \mathbf{q}$ , and the intensity will be a  $\mathbf{d}$ -Dirac.

Furthermore, during ball milling and heat treatments not only crystallite size is found to vary but also some strains may appear in the material which, to some extent, can deform the grains or particles. In general, it is important to distinguish between macrostrains, which affect the overall crystal, and microstrains, which are created by the influence of neighboring grains in the form of dislocations, stacking faults, etc. Both the crystallite size and microstrains can be evaluated from the width of the diffraction peaks. However, in the peak width there is also an experimental contribution. Therefore, in order to obtain reliable values of the crystallite size, all effects have to be somehow isolated and evaluated separately.

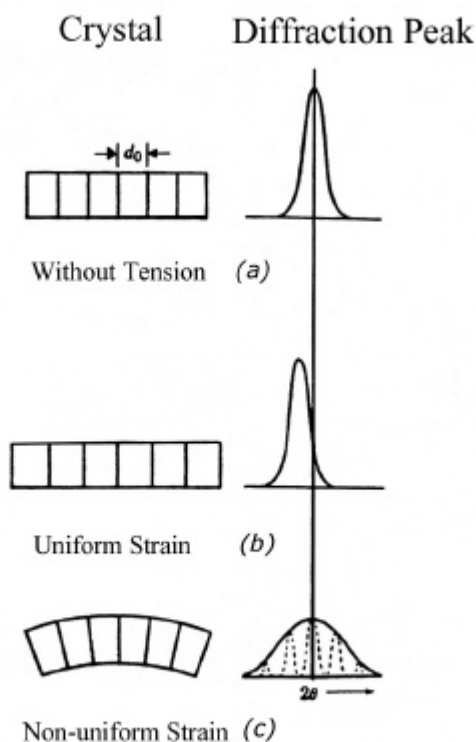


**Figure A1.3:** Effect of strains on the width and position of the diffraction peaks [1]

It is qualitatively easy to understand that microstrains contribute to broaden the diffraction peaks, while macrostrains induce a shift in their positions. Figure A1.3 shows schematic diagrams of (a) unstrained crystal, (b) uniformly strained crystal and (c) non-uniformly strained crystal. In (b) a macrostrain is shown to bring about an increase of the cell parameter, thus shifting the diffraction peak to a lower angle. In (c) the non-uniform strain makes different portions of the crystallites to deform differently. Thus, the cell parameter varies inside the crystallite from one region to another. As a result, we would obtain several sharp peaks (one from every sub-crystallite), mutually overlapped which, as a result, would give a wide diffraction peak, as observed experimentally.

### **I.III.- Evaluation of structural parameters by single-peak fit method (Marquardt Model)**

The analysis of XRD data can be performed by fitting peak by peak or fitting the whole spectra (Fourier analysis). The analysis peak by peak was carried out using the *MARQFITO* program, which was obtained from the Materials Engineering Department of

Trento University. This program fits the peaks using a *pseudo-Voigt* function, by means of mathematic algorithms, based on the *Marquardt model* [4], using a minimum square method.

The diffraction profile obtained experimentally,  $h(x)$ , is the convolution product of a “pure” diffraction profile,  $f(x)$ , and the experimental contribution,  $g(x)$ :

$$h(x) = \int_{-\infty}^{\infty} g(\mathbf{e}) f(x - \mathbf{e}) d\mathbf{e} \quad (\text{a1.11})$$

Crystallite sizes and microstrains are determined from the pure diffraction profile,  $f(x)$ . A good approximation of  $f(x)$  is obtained using a *pseudo-Voigt* function [5], which can be written as a lineal combination of a Cauchy (related to crystallite size) and Gaussian (related to microstrains) functions. The width of the experimental contribution to the diffraction peak,  $g(x)$ , also has these two components.

It has been demonstrated that the Voigt function is a good mathematical approach to describe the behavior of the diffraction peaks [6]. In particular, it can be written as the convolution product of a Gaussian,  $G(x)$ , and a Lorentzian (or Cauchy),  $C(x)$ , functions, which when normalized to the peak integrated intensities, are given by:

$$G(x) = \frac{2}{W_{1/2}} \sqrt{\frac{\ln 2}{\mathbf{P}}} \cdot \exp\left[-\frac{4 \ln 2}{W_{1/2}^2} x^2\right] \quad (\text{a1.12})$$

$$C(x) = \frac{2}{\mathbf{P}} \cdot \frac{1}{W_{1/2}} \cdot \left[ \frac{1}{1 + \frac{4x^2}{W_{1/2}^2}} \right] \quad (\text{a1.13})$$

where  $x$  represents the distance with respect to the maximum of the diffraction peak (it takes the value 0 at the peak center) and  $W_{1/2}$  is the full-width at half height, once the background is eliminated. Sometimes it is also designated as *HWHM* (*half width at half maximum*). It is necessary to distinguish  $W_{1/2}$  from the integral width,  $\mathbf{b}$ , which is defined as the integrated intensity of the peak divided by its height:

$$\mathbf{b} = \frac{1}{I_p} \int I(2\mathbf{q}) d(2\mathbf{q}) \quad (\text{a1.14})$$

where  $I_p$  is the maximum intensity of the peak and  $I(2\mathbf{q})$  is the intensity corresponding to the angle  $2\mathbf{q}$

Therefore, the instrumental function,  $g(x)$ , has two contributions: gaussian ( $g_G(x)$ ), which is mainly due to the x-rays source and geometry and is especially important for low angles ( $2\mathbf{q} < 90^\circ$ ), and the lorentzian ( $g_C(x)$ ), which is mainly due to the wavelength dispersion and is especially important for high angles. Therefore,  $g(x)$  can be written as the convolution product of  $g_G(x)$  and  $g_C(x)$ , which we can indicate in a simple way as follows:

$$g(x) = g_G(x) * g_C(x) \quad (\text{a1.15})$$

Similarly, the pure diffraction profile,  $f(x)$ , can be expressed as a convolution product of a gaussian contribution, due to microstrains, and a lorentzian contribution, due to crystallite size distribution. We can express, therefore,  $f(x)$  as follows:

$$f(x) = f_G(x) * f_C(x) \quad (\text{a1.16})$$

In summary, the experimental profile can be written in this way:

$$h(x) = [f_G(x) * g_G(x)] * [f_C(x) * g_C(x)] \quad (\text{a1.17})$$

To avoid having to calculate lengthily the integrals of the convolution product, a good approximation is to use the pseudo-Voigt function, instead of the Voigt function. The pseudo-Voigt function can be written as a linear combination of Cauchy and Gauss functions:

$$pV(x) = \mathbf{h}C(x) + (1 - \mathbf{h})G(x) \quad (\text{a1.18})$$

where  $\mathbf{h}$  is the Gaussian parameter, which can take values from 0 to 1. If  $\mathbf{h}$  is close to unity this indicates that the curve is lorentzian-like. Conversely if  $\mathbf{h}$  is close to 0, the gaussian contribution predominates. For  $x = 0$ , i.e. at the maximum intensity, the pseudo-Voigt function can be written in the following way:

$$pV(0) = \mathbf{h} \left( \frac{2}{\mathbf{p}} \right) \left( \frac{1}{W_{1/2}} \right) + (1 - \mathbf{h}) \left( 2\sqrt{\frac{\ln 2}{\mathbf{p}}} \right) \left( \frac{1}{W_{1/2}} \right) \quad (\text{a1.19})$$

Moreover, both the integral width and the full width at half height, are taken into account in the factor form parameter:

$$\Phi = \frac{2W_{1/2}}{\mathbf{b}} \quad (\text{a1.20})$$

Hence, it is possible to express the integral width as follows:

$$\mathbf{b} = \frac{2W_{1/2}}{\Phi} = \frac{\text{area}_{\text{peak}}}{I_p} = \frac{1}{pV(0)} \quad (\text{a1.21})$$

where the last equality is valid when the overall area of the peak is normalized to unity.

Therefore, the form factor gives an idea of the gaussian and lorentzian profile contributions, since it can be expressed in the following way:

$$\Phi = \left[ \left( \frac{\sqrt{\mathbf{p}}}{2\sqrt{\frac{\ln 2}{\mathbf{p}}}} \right) + \left( \frac{\mathbf{p}}{2} - \frac{\sqrt{\mathbf{p}}}{2\sqrt{\frac{\ln 2}{\mathbf{p}}}} \right) \mathbf{h} \right]^{-1} \quad (\text{a1.22})$$

This relationship holds both for the instrumental or the observed (experimental) profiles and, thus, it avoids having to work with the convolution products.

Experimentally, it has been demonstrated that the observed and experimental profiles fulfil the following relationships [5]:

$$\frac{\mathbf{b}_c}{\mathbf{b}} = a_0 + a_1\Phi + a_2\Phi^2 \quad (\text{a1.23})$$

$$\frac{\mathbf{b}_G}{\mathbf{b}} = b_0 + b_{1/2} \left( \Phi - \frac{2}{\mathbf{p}} \right)^{1/2} + b_1\Phi + b_2\Phi^2 \quad (\text{a1.24})$$

where the  $a$  and  $b$  parameters take the following values:

## Appendix I

$$\begin{aligned}
 a_0 &= 2.0207 & b_0 &= 0.6420 \\
 a_1 &= -0.4803 & b_{1/2} &= 1.4187 \\
 a_2 &= -1.7756 & b_1 &= -2.2043 \\
 & & b_2 &= 1.8706
 \end{aligned}$$

The error in this approach is estimated to be less than 1 %. Moreover, the following relationships are also valid:

$$\mathbf{b}_{hG}^2 = \mathbf{b}_{fG}^2 + \mathbf{b}_{gG}^2 \quad (\text{a1.25})$$

$$\mathbf{b}_{hC} = \mathbf{b}_{fC} + \mathbf{b}_{gC} \quad (\text{a1.26})$$

The values  $\mathbf{q}$ ,  $W_{1/2}$  and  $\mathbf{h}$  for the experimental spectra are determined using the fitting program. From equation a1.22 it is possible to determine the form factor of the observed spectra and from equation a1.21 the integral width,  $\mathbf{b}_h$ , can also be evaluated. Then, using equations a1.23 and a1.24 it is possible to calculate  $\mathbf{b}_{hC}$  and  $\mathbf{b}_{hG}$ . The instrumental values of  $W_{1/2}$  and  $\mathbf{h}$  were determined using a Si single-crystal standard and they were found to fulfil the following expressions:

$$\begin{aligned}
 1-\mathbf{h} &= 0.84220 - 6.6440 \cdot 10^{-3} (2\mathbf{q}) \\
 W_{1/2}^2 &= 1.8064 \cdot 10^{-4} + 1.3797 \cdot 10^{-3} \cdot \text{tg}(\mathbf{q}) + 7.6180 \cdot 10^{-4} \cdot (\text{tg}(\mathbf{q}))^2 \quad (\text{a1.27})
 \end{aligned}$$

Finally, expressions a1.25 and a1.26 can be used to determine the Cauchy,  $\mathbf{b}_{fC}$ , and Gaussian,  $\mathbf{b}_{gC}$ , contributions of the “pure” diffraction profile.

The Cauchy part of the integral width,  $\mathbf{b}_{fC}$ , is related to the microstrains, while the gaussian contribution,  $\mathbf{b}_{gC}$ , to the width is related crystallite size. Hence, for a specific peak, crystallite size is determined from  $\mathbf{b}_{fC}$  using the following expression:

$$d_{hkl} = \frac{\mathbf{l}}{\mathbf{b}_{fC} \cos \mathbf{q}_B} \quad (\text{a1.28})$$

where  $\mathbf{q}_B$  is the angular position of the peak (measured in radians) and  $\mathbf{l}$  is the wavelength (measured in Å). The value of  $d_{hkl}$  represents the diffraction coherent domain and is measured

also in Å. This formula is able to estimate crystallites sizes up to 1000 Å. For larger  $d_{hkl}$ ,  $\mathbf{b}_C$  tends to 0 and  $d_{hkl}$  to  $\infty$ . Equation a1.28 is called the *Scherrer formula*.

The following expression can be used to determine microstrains:

$$\text{microstrain} = \langle e \rangle = \frac{\mathbf{b}_{fG}}{4tg\mathbf{q}_B} \quad (\text{a1.29})$$

where  $\langle e \rangle$  represents the upper limit of microstrains. However, it is more frequent to use the mean square root of microstrains,  $\langle \mathbf{e}^2 \rangle^{1/2}$  (*rms strain*), which is related to  $\langle e \rangle$  in the following way:  $\langle e \rangle = 1.25 \langle \mathbf{e}^2 \rangle^{1/2}$ .

#### **L.IV.- The full pattern fit procedure: Rietveld Method**

The Rietveld method is used to obtain structural information of the sample by fitting the entire XRD pattern, thereby overcoming the problem of peak overlap and allowing the maximum amount of information to be extracted. In the Rietveld method, during the refinement process, structural parameters, background coefficients and profile parameters are varied in a least-squares procedure until the calculated powder profile, based on the structural model, best matches the observed pattern [7].

This method was first applied to powder neutron diffraction data but later it was adapted for use with x-ray data. A limitation of the Rietveld method is that one must start with a model that is a reasonable approximation of the actual structure and it is, therefore, primarily a structure refinement, as opposed to structure solution techniques. Rietveld refinements can yield very precise structural parameters, as well as quantitative analyses of phase mixtures.

The basic requirements for any Rietveld refinement are: accurate powder diffraction intensity data measured in intervals of  $2\mathbf{q}$  (i.e. step-scan), a starting model that is reasonably close to the actual crystal structure of the material of interest and a model that accurately describes shapes, widths and any systematic errors in the positions of the Bragg peaks in the powder pattern.

The calculation of all structural parameters, by means of the Rietveld method, has been carried out using the *MAUD* program, created by L. Lutterotti in Trento University [8]. Although it is out of the scope of this thesis to give a detailed description of all the equations

used by the program, in the following paragraphs some of the more relevant aspects of the way the program fits the data will be summarized.

During a Rietveld refinement, the quantity that is minimized by the least-squares procedure is the *weighted R-pattern*,  $R_{wp}$ , which is given by [7]:

$$R_{wp} = \left[ \frac{\sum_i w_i (Y_{io} - Y_{ic})^2}{\sum_i w_i Y_{io}^2} \right]^{1/2} \quad (\text{a1.30})$$

where  $Y_{io}$  is the observed intensity and  $Y_{ic}$  is the calculated intensity at step  $i$ , and  $w_i$  is the statistical weight assigned to each step intensity:

$$w_i = \mathbf{s}_i^2 = \mathbf{s}_{ig}^2 + \mathbf{s}_{ib}^2 \quad (\text{a1.31})$$

Here  $\mathbf{s}_b$  is the background standard deviation and  $\mathbf{s}_g$  is the standard deviation at each step  $i$  of the rest of the spectrum. The goodness of fit can be estimated from comparison of  $R_{wp}$  with the following parameter:

$$R_{\text{exp}} = \left[ \frac{N - P}{\sum_i w_i Y_{io}^2} \right]^{1/2} \quad (\text{a1.32})$$

where  $N$  is the number of points in the spectrum and  $P$  the number of parameters to be fitted. Usually the results are normalized and expressed in terms of  $GoF = R_{wp}/R_{\text{exp}}$ . If  $GoF$  would take a value equal to 1 it would indicate that the fit is perfect.

The calculated XRD profile,  $Y_c$ , can be expressed in the following way:

$$Y_c(2\mathbf{q}) = [B * I](2\mathbf{q}) + bkg \quad (\text{a1.33})$$

where  $B(2\mathbf{q})$  is the function that describes the sample profile,  $I(2\mathbf{q})$  is the instrumental profile and  $bkg$  is the background, which is fitted using a 4<sup>th</sup> degree polynomial. As in the *Marquardt model*  $B$  and  $I$  are fitted using a pseudo-Voigt function.

Actually, complicated algorithms are used to express  $B(2\mathbf{q})$ . For crystallite size and microstrains determination MAUD used the *Delft model* [7,9], which is based on the fact that

broadening due to crystallite size refinement does not change with  $2\theta$  while the microstrains contribution depends on  $2\theta$ . The program is also able to quantify stacking faults, based on Warren's formulae [10]. In brief, Warren's model takes into account the experimental observation that, for example, in a hexagonal close-packed phase, stacking faults make increase the widths for XRD peaks with Miller indexes  $(hkl)$  satisfying the following conditions:  $h - k = 3n + l$  (where  $n$  is an integer) and  $l = 0$  and, at the same time, they are responsible for the anomalous decrease of the relative intensity of peaks with  $l$  even. Moreover, MAUD is able to discern into two different types of stacking faults, namely deformation (due to slip) and twin (due to the formation of twins) stacking faults. Deformation stacking faults decrease slightly the intensity for peaks with  $l$  even and increase the intensity for peaks with  $l$  odd. The broadening due to deformation faults is the same for  $l$  even or odd, but the broadening due to twin faults is only one-third as large for  $l$  odd as for  $l$  even. The different effects of both types of faults into the diffractograms are taken into account in the full-pattern fitting procedure in order to quantify them. There are no peak displacements and no peak asymmetries as a result of either deformation or twin faults.

## References

- [1] B.D. Cullity, *Elements of X-Ray Diffraction*. (Addison-Wesley Publishing Company Inc., Boston, 1978).
- [2] W.L. Bragg, Proc. Camb. Phil. Soc. **17** (1912) 43.
- [3] P. Scherrer, Gött. Nachr. **2** (1918) 98.
- [4] D. W. Marquardt, J. Soc. Indust. Appl. Math. **11** (1963) 431.
- [5] T. H. Keijser, J. I. Landford, E. J. Mittemeijer, A. B. P. Vogels, J. Appl. Cryst. **15** (1982) 308.
- [6] S. Galí, Boletín de la Sociedad Castellonense de Cultura **LXV** (1989) 627.
- [7] R. A. Young, *The Rietveld Method* (International Union of Crystallography, Oxford University Press, 1995).
- [8] L. Lutterotti, P. Scardi, J. Appl. Cryst. **23** (1990) 246; L. Lutterotti, S. Gialanella, Acta Mater. **46** (1997) 101.
- [9] J. G. M. van Berkum, R. Deles, H. Th. de Keijser, E. J. Mittemeijer, Acta Cryst. **A52** (1996) 730.
- [10] B. E. Warren, *X-ray Diffraction* (Addison-Wesley, Reading, Massachusetts, 1969).

## APPENDIX -II-

### Macroscopic magnetic properties. Units

In the gaussian-cgs units system, with which our results will be given, the magnetic induction or magnetic flux density,  $\vec{B}$ , can be expressed by the following relationship [1]:

$$\vec{B} = \vec{H} + 4\pi\vec{M} \quad (\text{a2.1})$$

where  $\vec{B}$  is measured in Gauss (G),  $\vec{H}$  is the applied magnetic field and is measured in Oe and  $\vec{M}$  is the magnetization and is measured in emu / cm<sup>3</sup>.

The magnetization is defined as the ratio between the magnetic moment,  $m$ , and the volume,  $V$ , of the material:

$$M = \frac{m}{V} \quad (\text{a2.2})$$

Microscopic theories show that the dipolar magnetic moment, observed in bulk ferromagnetic materials, arises from two different contributions: it is, in part, due to the rotation of electrons around the atomic nucleus (orbital angular momentum) and also to the rotation of electrons around their own axis (spin angular momentum). The atomic nucleus has also a magnetic moment but it is so small compared to electronic magnetization that it is usually neglected in macroscopic magnetic measurements. In ferromagnetic materials, the magnetic moments align parallel to each other forming the so-called *magnetic domains* and the overall magnetic moment can be considered to be the sum of all the magnetic moments of every individual atom. In the gaussian units system  $|\vec{m}|$  is measured in erg / G or emu (electromagnetic unit).

Another common way to refer to the magnetic signal is the specific magnetization,  $\mathbf{s}$ , which is the ratio between the magnetic moment,  $m$ , and the mass,  $q$ :

$$\mathbf{s} = \frac{m}{q} = \frac{m}{V\rho} = \frac{M}{\rho} (\text{emu} / \text{g}) \quad (\text{a2.3})$$

where  $\rho$  is the density of the material.

The curve  $M$  versus  $H$  is called hysteresis loop. In general, in FM materials, these loops are symmetric and, therefore, the *coercivity*,  $H_C$ , is simply determined by the intersection of the curve with the magnetic field axis. However, as has been described in the introduction, in exchange coupled FM-AFM materials the loops become asymmetric, as shown in figure A2.1. In this case, the coercivity can be calculated from the values of  $H_{C1}$  and  $H_{C2}$ , i.e. the intersections both with the positive and negative field axis, using the following formula:

$$H_C = \left| \frac{H_{C1} - H_{C2}}{2} \right| \quad (\text{a2.4})$$

Similarly, the hysteresis loop shift is calculated as follows:

$$H_E = \frac{H_{C1} + H_{C2}}{2} \quad (\text{a2.5})$$

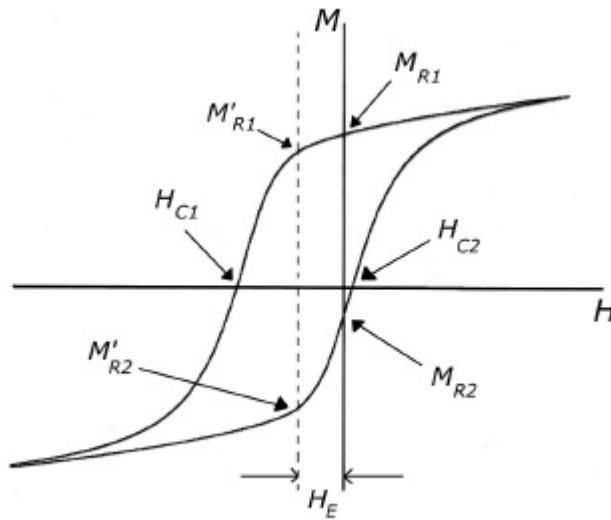


**Figure A2.1:** Schematic picture of a shifted hysteresis loop

As indicated in the introduction, the squareness ratio, which is defined as the ratio between the remanent and saturation magnetization,  $M_R/M_S$ , gives an idea of how square is the hysteresis loop. This magnitude, which is adimensional, has been determined after recentering

the hysteresis loop, i.e. removing the asymmetry by shifting it by the amount  $H_E$  along the magnetic field axis.

The remanence is then simply the average between  $M'_{R1}$  and  $M'_{R2}$ , which are the intersections of the curve with the ordinate (magnetization) axis of the hysteresis loop (see figure A2.1).

$$M_R = \frac{|M'_{R1}| + |M'_{R2}|}{2} \quad (\text{a2.6})$$

Determination of  $M_S$  has been carried out by the *law of approach to saturation* [1]:

$$M = M_S \left[ 1 - \frac{a}{H} - \frac{b}{H^2} \right] + cH \quad (\text{a2.7})$$

where  $a$  and  $b$  are magnetic coefficients that depend on the magnetic and structural properties of the material and  $c$  is the magnetic susceptibility. The parameter  $a$  is considered to be related to demagnetizing effects and inhomogeneities of the material (grain boundaries, dislocations, non-magnetic inclusions) while  $b$  is related to the magnetic anisotropy and magnetostriction of the material.

In a close magnetic circuit the magnetostatic energy stored in the system can be expressed as:

$$U = \frac{1}{2} \int_V (\vec{B} \cdot \vec{H}) dV \quad (\text{a2.8})$$

The quality of a permanent magnet, which is determined by the energy that it can store, can be estimated from the product  $\vec{B} \cdot \vec{H}$ . This product is not only a material property but it also depends on the considered point of the hysteresis loop. Figure A2.2 shows the so-called *demagnetization curve*, which is the second quadrant of the hysteresis loop. It can be seen in the figure that at the point  $A'$  the value of  $\vec{B}$  is quite high. However, the value of  $\vec{H}$  at this point is small. Conversely, the point  $A''$  has a high value of  $\vec{H}$  but  $\vec{B}$  is small. Therefore it is much better to work on point  $A$ , where  $\vec{B} \cdot \vec{H}$  takes its maximum value, which is commonly referred to as  $(BH)_{Max}$ . In order to have high  $(BH)_{Max}$  there are three necessary requirements: to have high  $M_S$ , a large  $H_C$  and a loop as square as possible, i.e.  $M_R/M_S$  as close to 1 as possible.

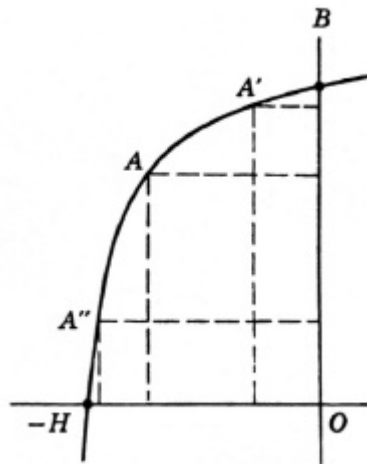


**Figure A2.2:** Demagnetization curve of a permanent magnetic material.

From the hysteresis loop the value of  $(BH)_{Max}$  can be obtained by plotting the product  $(B.H)$  as a function of  $B$  and estimating the maximum of the curve. In our particular case it is necessary to re-center the hysteresis loop before doing such a representation.

## References

- [1] S. Chikazumi, *Physics of Magnetism*. (John Wiley & Sons Inc., New York, 1964).